AIP Applied Physics Letters

# High performance In2O3 thin film transistors using chemically derived aluminum oxide dielectric

Pradipta K. Nayak, M. N. Hedhili, Dongkyu Cha, and H. N. Alshareef

Citation: Applied Physics Letters **103**, 033518 (2013); doi: 10.1063/1.4816060
View online: http://dx.doi.org/10.1063/1.4816060
View Table of Contents: http://scitation.aip.org/content/aip/journal/apl/103/3?ver=pdfcov
Published by the AIP Publishing

**Articles you may be interested in**

Oxygen plasma assisted high performance solution-processed Al2Ox gate insulator for combustion-processed InGaZnOx thin film transistors
J. Appl. Phys. **117**, 035703 (2015); 10.1063/1.4906107

The effects of buffer layers on the performance and stability of flexible InGaZnO thin film transistors on polyimide substrates
Appl. Phys. Lett. **104**, 063508 (2014); 10.1063/1.4864617

Low-voltage InGaZnO thin-film transistors with Al 2 O 3 gate insulator grown by atomic layer deposition
Appl. Phys. Lett. **94**, 142107 (2009); 10.1063/1.3118575

High-performance InGaZnO thin-film transistors with high- k amorphous Ba 0.5 Sr 0.5 Ti O 3 gate insulator
Appl. Phys. Lett. **93**, 242111 (2008); 10.1063/1.3054335

GaN metal-oxide-semiconductor high-electron-mobility-transistor with atomic layer deposited Al 2 O 3 as gate dielectric
Appl. Phys. Lett. **86**, 063501 (2005); 10.1063/1.1861122

This article is copyrighted as indicated in the article. Reuse of AIP content is subject to the terms at: http://scitation.aip.org/termsconditions. Downloaded to IP: 109.171.137.210 On: Tue, 05 May 2015 12:11:11

APPLIED PHYSICS LETTERS **103**, 033518 (2013)

# High performance $In_2O_3$ thin film transistors using chemically derived aluminum oxide dielectric

Pradipta K. Nayak,[1] M. N. Hedhili,[2] Dongkyu Cha,[2] and H. N. Alshareef[1,a)]
[1]*Materials Science and Engineering, King Abdullah University of Science and Technology (KAUST), Thuwal 23955-6900, Saudi Arabia*
[2]*Imaging and Characterization Laboratory, King Abdullah University of Science and Technology (KAUST), Thuwal 23955-6900, Saudi Arabia*

(Received 8 June 2013; accepted 1 July 2013; published online 18 July 2013)

We report high performance solution-deposited indium oxide thin film transistors with field-effect mobility of 127 $cm^2/Vs$ and an $I_{on}/I_{off}$ ratio of $10^6$. This excellent performance is achieved by controlling the hydroxyl group content in chemically derived aluminum oxide ($AlO_x$) thin-film dielectrics. The $AlO_x$ films annealed in the temperature range of 250–350 °C showed higher amount of Al-OH groups compared to the films annealed at 500 °C, and correspondingly higher mobility. It is proposed that the presence of Al-OH groups at the $AlO_x$ surface facilitates unintentional Al-doping and efficient oxidation of the indium oxide channel layer, leading to improved device performance. © *2013 AIP Publishing LLC*. [http://dx.doi.org/10.1063/1.4816060]

Over the past 10 years, transparent oxide thin film transistors (TFTs) have been extensively studied due to their potential use in large area flat-panel display (FPD) applications. Oxide semiconductor based TFTs have been proven to be the alternative candidates to the low mobility silicon-based TFTs, which are currently being used for display applications.[1] High performance oxide TFTs have been reported using vacuum deposition techniques[2–5] and have also been used for the demonstration of display devices.[6,7] Solution deposition techniques have also been employed for the fabrication of oxide TFTs. During the last few years, zinc oxide,[8,9] indium oxide,[10,11] zinc tin oxide,[12,13] indium zinc oxide,[14,15] and indium gallium zinc oxide[16–18] based thin film transistors with reasonable performance have been reported using spin coating technique. It is noted that, in most of the previously reports on solution processed TFTs, high annealing temperatures have been used to achieve better device performances and the TFTs are operated in very high operating voltage ranges. In practical, however, TFTs prepared at low processing temperatures with high field-effect mobility, high $I_{on}/I_{off}$ ratio, low turn-on voltage, and small sub-threshold swing values are needed for low-voltage operation and faster switching applications. The use of appropriate metal precursors, solvents, and appropriate gate dielectric are very crucial parameters to enable low process temperatures and good device performances. Low voltage operated TFTs with good performance have been reported using solution-processed gate dielectrics such as zirconium oxide[13] and sodium beta-alumina.[19] However, the processing temperature of typical dielectric layers is very high in these cases (>500 °C), which is not suitable to be used for practical display applications.

In the present work, we demonstrated the fabrication of high performance and low-voltage operated TFTs using solution processed $In_2O_3$ as the semiconducting layer and aluminium oxide ($AlO_x$) as the gate dielectrics at significantly lower temperature. We found that the aluminium hydroxide content present in spin coated aluminium oxide dielectrics plays an important role to obtain high performance $In_2O_3$ TFTs.

The precursor solution for the preparation of $AlO_x$ films was prepared by dissolving aluminum chloride (0.5 M) in a mixture of acetonitrile (AN) and ethylene glycol (EG) with AN to EG ratio of 3:7. The mixed solutions were stirred at room temperature in air for 4 h. Heavily doped p-type silicon wafers were used as the gate electrode and substrate. The Si substrates were cleaned ultrasonically by ethanol, acetone, and isopropanol and then exposed to oxygen plasma for 2 min to enhance the hydrophilicity. The $AlO_x$ precursor solution was spun on the cleaned Si surfaces at a rotation speed of 3000 rpm in air. After spin coating, the wet films were placed on a hot plate at 90 °C for 5 min and then subjected to rapid annealing at the temperature range of 250-500 °C in air for 10 min. The spin coating and annealing process was repeated for three times. Finally, the $AlO_x$ films were annealed in the temperature range of 250-500 °C for 2 h in air. The $AlO_x$ films prepared at 250 °C, 350 °C, and 500 °C, hereafter will be called as $AlO_x$-250 °C, $AlO_x$-350 °C, and $AlO_x$-500 °C, respectively. The average thickness of the $AlO_x$-250 °C, $AlO_x$-350 °C, and $AlO_x$-500 °C were found to be ~120 nm, ~115 nm, and ~95 nm, respectively. Indium chloride (0.05 M) dissolved in acetonitrile and ethylene glycol (9:1 v/v) was used as the precursor solution for the preparation of $In_2O_3$ semiconductor channel layer. The mixed solution was stirred at ~50 °C for 1 h. One layer of the indium oxide precursor solution was spun on $AlO_x$ films at a rotation speed of 4000 rpm in air. The wet films were kept on a hot plate at 80 °C for 5 min and then subjected to rapid annealing at 250 °C for 1 h in air using a tube furnace. Circular shaped aluminum contacts (thickness ~80 nm) with diameter of 100 $\mu$m were used for the capacitance and leakage current measurements of the $AlO_x$ films. Aluminum source and drain electrodes with channel width to length ratio (W/L) of 10 (W = 1000 $\mu$m and L = 100 $\mu$m) were used for the transistor characteristic measurements. The aluminum contacts were deposited using shadow mask and e-beam evaporation. Crystallinity of the $AlO_x$ and $In_2O_3$ films were studied by x-ray diffraction (XRD) diffractometer (Bruker D8

a)Author to whom correspondence should be addressed. Electronic mail: husam.alshareef@kaust.edu.sa

 © 2013 AIP Publishing LLC

This article is copyrighted as indicated in the article. Reuse of AIP content is subject to the terms at: http://scitation.aip.org/termsconditions. Downloaded to IP: 109.171.137.210 On: Tue, 05 May 2015 12:11:11

Discover) using Cu *Kα* radiation. The chemical composition of the $AlO_x$ and $In_2O_3$ films were analyzed by x-ray photoelectron spectroscopy (XPS) using an Axis Ultra DLD spectrometer (Kratos Analytical, UK). Capacitance of the $AlO_x$ films was measured by a Precision LCR meter (Agilent E4980A). The current-voltage characteristics of the $AlO_x$ capacitors and $In_2O_3$ TFTs were performed using a semiconductor characterization system (Keithley 4200-SCS).

The x-ray diffraction (XRD) patterns of the $AlO_x$ films prepared at different annealing temperatures are shown in Fig. 1(a). No peak corresponding to the crystalline $Al_2O_3$ was observed, suggesting amorphous $AlO_x$ films were obtained over the entire range of annealing temperatures. The AFM images of the corresponding $AlO_x$ films are shown in Figs. 1(b)–1(d). The interface roughness of the gate dielectric is one of the crucial parameter to reduce carrier scattering and obtain high field-effect mobility. The root mean square surface roughness of the $AlO_x$-250 °C, $AlO_x$-350 °C, and $AlO_x$-500 °C was measured to be 0.3 nm, 0.2 nm, and 0.2 nm, respectively, and the obtained low surface roughness values are ideal for obtaining good device performances.

The chemical composition of the $AlO_x$ films was investigated by XPS measurements. The XPS O1s peaks of the $AlO_x$ films prepared at different annealing temperatures are shown in Fig. 2(a). The open circles show the measured data and the solid lines represents the Gaussian peak fitting results. The deconvoluted results of O1s peaks exhibited a peak at ~531.0 eV, attributed to the $O^{-2}$ in $Al_2O_3$ and another peak at ~532.3 eV, attributed to oxygen associated to the $OH^-$ in aluminum hydroxide.[20] The intensity of the two peaks at ~531.0 eV and ~532.3 eV were comparable in case of $AlO_x$-250 °C. Interestingly, the intensity of the peak at ~532.3 eV decreased and subsequently, the intensity of the peak at ~531.0 eV increased with increasing annealing temperature above 250 °C. The decreased intensity of the peak at ~532.3 eV may be attributed to the conversion of more aluminum hydroxides to form $Al_2O_3$ at higher temperatures. It may be noted here that the associated OH groups are mainly

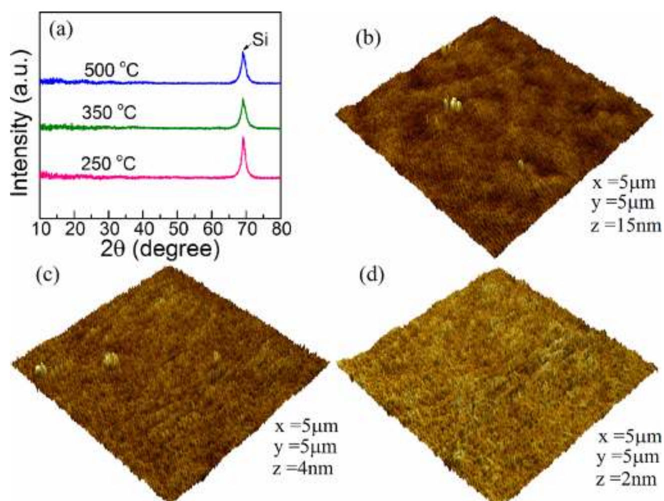


FIG. 1. (a) XRD patterns of $AlO_x$ films prepared at different annealing temperatures and AFM images of $AlO_x$ films prepared at (b) 250 °C, (c) 350 °C, and (d) 500 °C.

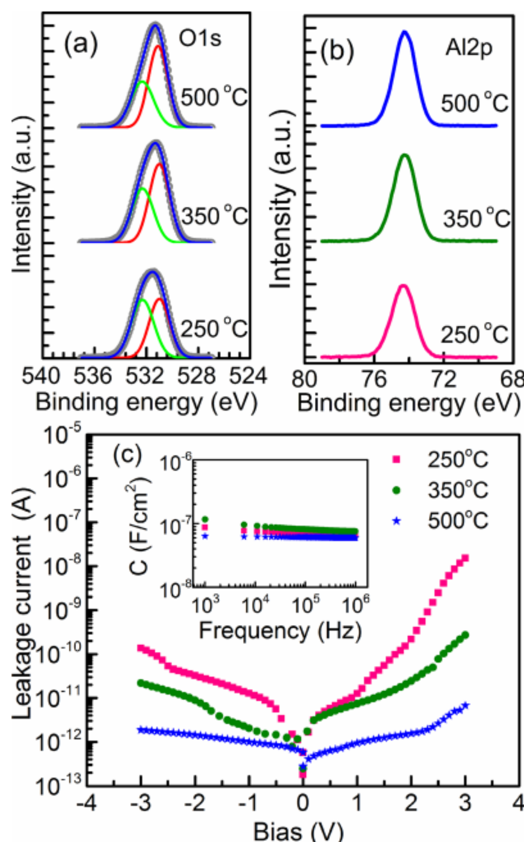


FIG. 2. XPS (a) O1s and (b) Al2p spectra of $AlO_x$ films prepared at different annealing temperatures. (c) Leakage current *vs* voltage and capacitance vs frequency curves (inset) of $AlO_x$ films prepared at different annealing temperatures measured with $p^+$-Si/AlOx/Al structures.

due to the water absorbed from the environment in the AlOx films after the final annealing. At low annealing temperatures, all the aluminum atoms are not completely oxidized and hence they absorb water molecules from the environment to form aluminum hydroxides. Fig. 2(b) shows the Al2p peaks of the $AlO_x$ films prepared at different annealing temperatures. The XPS spectra show a singlet Al2p peak at ~74.3 eV in case of $AlO_x$-250 °C and $AlO_x$-350 °C, whereas, it was shifted to 74.2 eV in case of $AlO_x$-500 °C. The shifting of the Al2p peak towards lower binding energy in case of $AlO_x$-500 °C may be attributed to the decrease in the concentration of $OH^-$ ions or coordination number of $Al^{3+}$ ions in the film.[21] Fig. 2(c) shows the leakage current of different $AlO_x$ films measured with $p^+$-Si/$AlO_x$/Al structures. It is clearly seen that the leakage current of the $AlO_x$ films was decreased with increasing annealing temperature. The capacitance of the aforementioned $p^+$-Si/$AlO_x$/Al structures were measured in the frequency range of 1 kHz to 1 MHz and the obtained curves are shown in the inset of Fig. 2(c). The measured capacitance at 1 MHz for $AlO_x$-250 °C, $AlO_x$-350 °C, and $AlO_x$-500 °C were found to be 66 nF/cm$^2$, 75 nF/cm$^2$, and 58 nF/cm$^2$, respectively. The high value of capacitance in case of the low temperature annealed $AlO_x$ films may attribute to the presence of OH-groups.[22]

The schematic of the TFT structure used in this work is shown in Fig. 3(a). Figs. 3(c)–3(e) show the out-put characteristics of the fabricated $In_2O_3$ TFTs using $AlO_x$-250 °C, $AlO_x$-350 °C, and $AlO_x$-500 °C as the gate dielectrics. The

This article is copyrighted as indicated in the article. Reuse of AIP content is subject to the terms at: http://scitation.aip.org/termsconditions. Downloaded to IP: 109.171.137.210 On: Tue, 05 May 2015 12:11:11

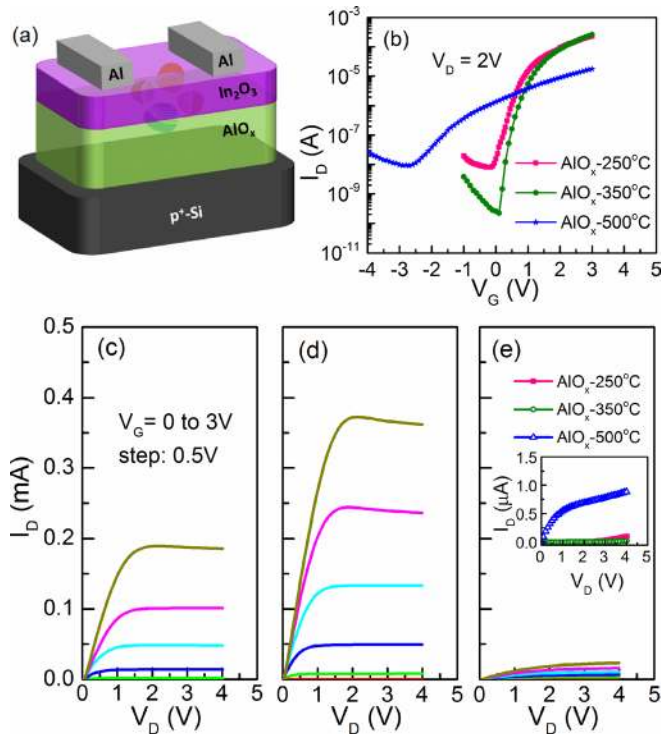


FIG. 3. (a) Schematic of the TFT structure, (b) transfer characteristic curves of the $In_2O_3$ TFTs fabricated using $AlO_x$ films prepared at different temperatures as the gate dielectrics. Out-put characteristic curves of the $In_2O_3$ TFTs fabricated using (c) $AlO_x$-250 °C, (d) $AlO_x$-350 °C, and (e) $AlO_x$-500 °C as the gate dielectrics. The inset in (e) shows the $I_D$ *vs* $V_D$ curves measured at zero gate voltage for the TFTs fabricated using $AlO_x$ dielectrics annealed at different temperatures.

out-put characteristics of the TFTs fabricated on $AlO_x$-250 °C and $AlO_x$-350 °C exhibited clear pinch-off and excellent hard saturation. Lower drain currents were obtained in case of the TFTs fabricated using $AlO_x$-500 °C as the gate dielectric and the TFTs were found to operate in the depletion mode operation with high negative turn-on voltage ($V_{on}$), which is the gate voltage at the onset of the initial sharp rise in drain current in a log ($I_D$)-$V_G$ transfer characteristic curve. The transfer characteristic curves of all the TFTs obtained at a constant drain to source voltage ($V_D$) of 2 V are shown in Fig. 3(b). The field-effect mobility ($\mu_{sat}$) of the TFTs was estimated in the saturation regime of the transfer curve (Fig. 3(b)) using the following equation:

$$I_{D,sat} = \frac{W}{2L}\mu_{sat}C_{ox}(V_G - V_{TH})^2, \quad (1)$$

where $I_D$ is the drain to source current, $V_G$ is the gate to source voltage, $V_{TH}$ is the threshold voltage, W and L are the channel width and length, respectively, and $C_{ox}$ is the capacitance per unit area of the gate dielectric. The values of $\mu_{sat}$ were found to be 82 $cm^2\,V^{-1}\,s^{-1}$ and 127 $cm^2\,V^{-1}\,s^{-1}$ for the $In_2O_3$ TFTs fabricated on $AlO_x$-250 °C and $AlO_x$-350 °C, respectively. The values of $V_{on}$ for the TFTs fabricated on $AlO_x$-250 °C and $AlO_x$-350 °C were found to be −0.1 V and 0.1 V, respectively. The drain off-current to on-current ratio ($I_{on}/I_{off}$) for the TFTs fabricated on $AlO_x$-250 °C and $AlO_x$-350 °C were $3 \times 10^4$ and $1 \times 10^6$, respectively. The low $I_{on}/I_{off}$ ratio in case of the TFTs fabricated on $AlO_x$-250 °C can be attributed to high leakage of

TABLE I. Electrical parameters of $In_2O_3$ TFTs fabricated using $AlO_x$ films annealed at different temperatures as the gate dielectrics.

| $AlO_x$ annealing temperature | $\frac{O_V}{O_V + O_L}$ | $\mu_{sat}$ ($cm^2$/Vs) | $I_{on}/I_{off}$ | $V_{on}$ (V) | SS (V/dec) |
|---|---|---|---|---|---|
| 250 °C | 24% | 82 | $3 \times 10^4$ | −0.1 | 0.271 |
| 350 °C | 28% | 127 | $1 \times 10^6$ | 0.1 | 0.137 |
| 500 °C | 31% | 5 | $2 \times 10^3$ | −2.6 | 0.951 |

$AlO_x$-250 °C as evident from the *I-V* curve shown in Fig. 2(c). As seen from Table I, the TFTs fabricated using $AlO_x$-500 °C as the gate dielectric showed very inferior performance compared to the TFTs fabricated on $AlO_x$-250 °C and $AlO_x$-350 °C.

Material characterizations of the $In_2O_3$ films were performed to understand the effect of annealing temperature of $AlO_x$ thin film dielectrics on the performance of $In_2O_3$ TFTs. The crystallinity of the $In_2O_3$ films was investigated by XRD using grazing incidence geometry with an incident angle of 1°. The grazing incidence XRD patterns (Fig. 4(a)) of the $In_2O_3$ films deposited on different $AlO_x$ films showed a broad peak at ∼30.5° corresponding to the (222) plane of $In_2O_3$. The Gaussian peak fitting of the observed peaks revealed that the full width at half maximum (FWHM) for the $In_2O_3$ films deposited on $AlO_x$-250 °C (FWHM = 2.5°) and $AlO_x$-350 °C (FWHM = 2.8°) are higher than that of the $In_2O_3$ film deposited on $AlO_x$-500 °C (FWHM = 2.1°). Furthermore, Fig. 4(b) shows the XPS O1s spectra of the $In_2O_3$ films deposited on $AlO_x$ films annealed at different temperatures. The Gaussian fitting (solid lines) of the all the O1s peaks exhibited a strong peak at 529.8 eV along with two shoulder peaks at 531.1 eV and 532.3 eV. The peak at 529.8 eV is attributed to the oxygen in $In_2O_3$ lattice without oxygen vacancy ($O_L$).[23] The peaks at 531.1 eV and 532.3 eV are attributed to the oxygen in $In_2O_3$ lattice with oxygen vacancy ($O_V$) and the OH groups attached to indium ions, respectively.[17,23] Interestingly, as shown in Table I, the ratio of $O_V/O_L+O_V$ is higher in case of the $In_2O_3$ film deposited on $AlO_x$-500 °C compared to the

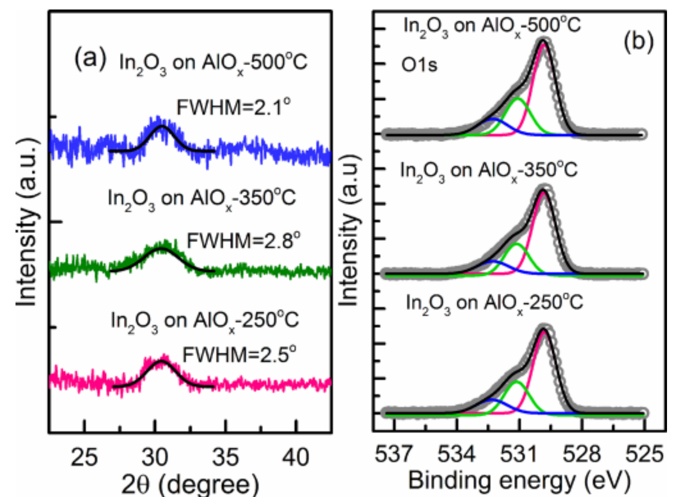


FIG. 4. (a) XRD patterns and (b) O1s XPS spectra of the $In_2O_3$ films deposited on $AlO_x$ films prepared at different annealing temperatures.

This article is copyrighted as indicated in the article. Reuse of AIP content is subject to the terms at: http://scitation.aip.org/termsconditions. Downloaded to IP: 109.171.137.210 On: Tue, 05 May 2015 12:11:11

$In_2O_3$ films deposited on $AlO_x$-250 °C and $AlO_x$-350 °C, indicating the presence of smaller concentration of oxygen vacancies in the latter two cases.

It is interesting to discuss the origin of the observed broadness of the XRD peaks and lower oxygen vacancy concentration in $In_2O_3$ films deposited on the $AlO_x$-250 °C and $AlO_x$-350 °C dielectrics. First, the XRD peak broadening most likely comes from the development of a more amorphous-like structure, a trend which has been previously reported for Al-doped $In_2O_3$ films,[11] possibly owing to the big difference between the atomic radii of Al (1.43 Å) and In (1.66 Å).[24] Thus, we suggest that the XRD peak broadening in case of $In_2O_3$ films deposited on $AlO_x$-250 °C and $AlO_x$-350 °C films is likely due to Al diffusion into the $In_2O_3$ channel from the underlying $AlO_x$ films that are rich Al-OH groups. Second, the OH-groups attached to the Al at the interface of $AlO_x$ as seen from the XPS O1s spectra (Fig. 2(a)) can act as oxygen source and induce a more efficient oxidation of $In_2O_3$ after annealing at 250 °C. Both Al-doping and OH-assisted oxidation of $In_2O_3$ are expected reduce the oxygen vacancy concentration in $In_2O_3$ films deposited on $AlO_x$-250 °C and $AlO_x$-350 °C films.[11,25] In contrast, higher oxygen vacancy concentration is expected in the $In_2O_3$ deposited on $AlO_x$-500 °C due to the reduced OH group concentration in $AlO_x$-500 °C (see XPS in Fig. 2(a)). This is also expected to increase the carrier concentration and conductivity of $In_2O_3$, which is believed to be controlled by oxygen vacancies.[26] The increased carrier concentration of $In_2O_3$ TFTs made on AlOx-500 °C is indeed observed as can be seen from the plot of drain current *vs* drain voltage measured at zero gate bias, as shown in the inset of Fig. 3(e). Fig. 3(e) shows significantly higher drain current in $In_2O_3$ TFTs made on AlOx-500 °C compared to the TFTs made on $AlO_x$-250 °C and $AlO_x$-350 °C dielectrics. The values of sub-threshold swing ($SS = \partial V_{DS}/\partial \log_{10} I_{DS}$) were found to be 0.271 V $dec^{-1}$, 0.137 V $dec^{-1}$, and 0.951 V $dec^{-1}$ for the TFTs fabricated on $AlO_x$-250 °C, $AlO_x$-350 °C, and $AlO_x$-500 °C, respectively. The high value of "*SS*" in case of the TFTs made on $AlO_x$-500 °C, further confirms the increased carrier concentration in $In_2O_3$ deposited on AlOx-500 °C. Thus, the inferior performance in case of the $In_2O_3$ TFT fabricated using AlOx-500 °C as the gate dielectric can be attributed to the scattering of carriers[18] due to the high carrier concentration in the corresponding $In_2O_3$ semiconductor layer. Hence, we find that the presence of Al-OH groups in low temperature annealed $AlO_x$ film plays a crucial role in $In_2O_3$ TFT performance. It is noted that the performance of our devices are superior to that of previously reported results for the solution processed $In_2O_3$ TFTs.[10,11,27]

In summary, thin film transistors were fabricated using solution-processed $In_2O_3$ semiconductor as the channel layer and $AlO_x$ films annealed at different temperatures as the gate dielectrics. The TFTs were operated at very low voltage range and exhibited better performance than previously reported $In_2O_3$ TFTs processed at these temperatures. High performance $In_2O_3$ TFTs could be obtained at relatively low processing temperatures by controlling the Al-OH content in solution processed $AlO_x$ gate dielectrics.

The authors acknowledge the generous support of the KAUST baseline fund.

[1]A. Facchetti and T. J. Marks, *Transparent Electronics: From Synthesis to Applications* (Wiley, 2010).
[2]E. M. C. Fortunato, P. M. C. Barquinha, A. C. M. B. G. Pimentel, A. M. F. Goncalves, A. J. S. Marques, L. M. N. Pereira, and R. F. P. Martins, Adv. Mater. **17**, 590 (2005).
[3]L. Wang, M. H. Yoon, A. Facchetti, and T. J. Marks, Adv. Mater. **19**, 3252 (2007).
[4]P. Barquinha, L. Pereira, G. Goncalves, R. Martins, and E. Fortunato, J. Electrochem. Soc. **156**, H161 (2009).
[5]J. S. Park, K. Kim, Y. G. Park, Y. G. Mo, H. D. Kim, and J. K. Jeong, Adv. Mater. **21**, 329 (2009).
[6]T. Kamiya, K. Nomura, and H. Hosono, Sci. Technol. Adv. Mater. **11**, 044305 (2010).
[7]T. Sakai, H. Seo, S. Aihara, M. Kubota, N. Egami, D. P. Wang, and M. Furuta, Jpn. J. Appl. Phys. **51**, 010202 (2012).
[8]B. S. Ong, C. S. Li, Y. N. Li, Y. L. Wu, and R. Loutfy, J. Am. Chem. Soc. **129**, 2750 (2007).
[9]P. K. Nayak, J. Jang, C. Lee, and Y. Hong, Appl. Phys. Lett. **95**, 193503 (2009).
[10]S. Y. Han, G. S. Herman, and C. H. Chang, J. Am. Chem. Soc. **133**, 5166 (2011).
[11]Y. H. Hwang, J. H. Jeon, K. J. Seo, and B. S. Bae, Electrochem. Solid-State Lett. **12**, H336 (2009).
[12]P. K. Nayak, J. V. Pinto, G. Goncalves, R. Martins, and E. Fortunato, J. Disp. Technol. **7**, 640 (2011).
[13]C. G. Lee and A. Dodabalapur, Appl. Phys. Lett. **96**, 243501 (2010).
[14]D. H. Lee, Y. J. Chang, G. S. Herman, and C. H. Chang, Adv. Mater. **19**, 843 (2007).
[15]K. K. Banger, Y. Yamashita, K. Mori, R. L. Peterson, T. Leedham, J. Rickard, and H. Sirringhaus, Nature Mater. **10**, 45 (2011).
[16]P. K. Nayak, T. Busani, E. Elamurugu, P. Barquinha, R. Martins, Y. Hong, and E. Fortunato, Appl. Phys. Lett. **97**, 183504 (2010).
[17]S. Jeong, J. Y. Lee, S. S. Lee, S. W. Oh, H. H. Lee, Y. H. Seo, B. H. Ryu, and Y. Choi, J. Mater. Chem. **21**, 17066 (2011).
[18]P. K. Nayak, M. N. Hedhili, D. K. Cha, and H. N. Alshareef, Appl. Phys. Lett. **100**, 202106 (2012).
[19]B. N. Pal, B. M. Dhar, K. C. See, and H. E. Katz, Nature Mater. **8**, 898 (2009).
[20]J. V. D. Brand, W. G. Sloof, H. Terryn, and J. H. W. de Wit, Surf. Interface Anal. **36**, 81 (2004).
[21]T. Tsuchida and H. Takahashi, J. Mater. Res. **9**, 2919 (1994).
[22]N. Biswas, J. A. Lubguban, and S. Gangopadhyay, Appl. Phys. Lett. **84**, 4254 (2004).
[23]R. Wan, M. Yang, Q. Zhou, and Q. Zhanga, J. Vac. Sci. Technol. A **30**, 061508 (2012).
[24]L. Pauling, J. Am. Chem. Soc. **69**, 542 (1947).
[25]Y. H. Kim, J. S. Heo, T. H. Kim, S. Park, M. H. Yoon, J. Kim, M. S. Oh, G. R. Yi, Y. Y. Noh, and S. K. Park, Nature **489**, 128 (2012).
[26]K. Nomura, T. Kamiya, H. Ohta, M. Hirano, and H. Hosono, Appl. Phys. Lett. **93**, 192107 (2008).
[27]H. S. Kim, P. D. Byrne, A. Facchetti, and T. J. Marks, J. Am. Chem. Soc. **130**, 12580 (2008).

This article is copyrighted as indicated in the article. Reuse of AIP content is subject to the terms at: http://scitation.aip.org/termsconditions. Downloaded to IP: 109.171.137.210 On: Tue, 05 May 2015 12:11:11